**Supplementary Material for**

# Extracting Charge and Mass Information from Highly Congested Mass Spectra Using Fourier-Domain Harmonics

Sean P. Cleary[1], Huilin Li[3], Dhanashri Bagal[2], Joseph A. Loo[3], Iain D.G. Campuzano[4], and James S. Prell[1,5]*

1. *Department of Chemistry and Biochemistry, 1253 University of Oregon, Eugene, OR 97403-1253, United States*
2. *Amgen Discovery Research, Amgen, Inc., 1120 Veterans Blvd, South San Francisco, CA 94080, United States*
3. *Department of Chemistry and Biochemistry, Department of Biological Chemistry, UCLA/DOE Institute for Genomics and Proteomics, University of California, Los Angeles, Los Angeles, CA 90095, United States*
4. *Molecular Structure and Characterization, Amgen, Inc., Thousand Oaks, CA 91320, United States*
5. *Materials Science Institute, 1252 University of Oregon, Eugene, OR 97403-1252, United States*

Submitted to *Journal of the American Society for Mass Spectrometry*

on 21 March 2018, revised 30 May 2018

Keywords: Native Mass Spectrometry, Nanodisc, Fourier Transform, Deconvolution

*Correspondence should be addressed to jprell@uoregon.edu

Tel: (541) 346-2597  Fax: (541) 346-4643

**Methods**

Native electrospray ionization mass spectrometry instrumental conditions. Orbitrap-EMR (Amgen, Thousand Oaks, CA, USA). Experiments were performed on a modified Exactive Plus instrument (ThermoFisher Scientific, Bremen, Germany) equipped with a nanoelectrospray ionization (nESI) source. All critical instrument voltages and pressures were as follows: The capillary voltage 0.8-1.5 kV. Ions formed by nESI were transmitted through a heated stainless steel capillary (4.25 cm long ion transfer tube) maintained at 200 °C into an S-Lens stacked ring ion guide with an applied RF-amplitude (peak-to-peak) of 200 V. Ions then traveled through a transport multipole and entered the HCD cell where they were stored at high pressure before they were returned to the C-trap. This feature allows efficient trapping and desolvation of large protein ions and dramatically improves sensitivity. Nitrogen gas was used in the C-trap as well as the HCD cell. Using a trapping gas pressure setting of 7.0 (software-determined) the C-trap pressure was approximately $2\times10^{-4}$ mbar and the UHV pressure (Orbitrap analyser) was $7.5\times10^{-10}$ mbar. The voltage offsets on the transport multipoles were manually tuned to increase the transmission of large complexes (C-trap entrance lens; 0 V, bent flatapole DC, 4 V; inter-flatapole DC 4 V; injection flatapole DC, 4 V). An in-source CID voltage of 50 V to 120 V and an HCD voltage of 20 V to 100 V were required to achieve efficient sample desolvation. Raw transients were processed using enhanced Fourier Transform [48] for converting the time-domain data into frequency before *m*/*z* conversion; this data pre-processing is standard for this generation of Orbitrap instruments. The instrument was set at a nominal resolving power of 70,000 at *m*/*z* 200, and mass spectra were acquired for 2 minutes by averaging 10 microscans per analytical scan. Data were analyzed using XcaliburTM2.2. No additional data processing was performed before Fourier-Transform analysis.

Quadrupole–Time-of-Flight mass analyzer (University of Oregon, Eugene, OR, USA). All QTOF mass spectrometry experiments, other than those shown in Supplementary Figure S3, were performed with a Synapt G2-S*i* ion mobility mass spectrometer (Waters Corp. Milford, MA, USA) using a static nESI source. nESI emitters were prepared by pulling borosilicate capillaries (i.d. 0.78 mm, Sutter Instruments) to a tip i.d. of ~1 μm using a Flaming-Brown P-97 micropipet puller (Sutter Instruments, Novato, CA, USA). For each sample, ~3−5 μL of solution was loaded into an emitter, which was placed approximately 1-2 mm from the entrance of the mass spectrometer. A platinum wire inserted into the solution was used to apply an electrical potential of 0.6-1.0 V relative to instrumental ground to initiate electrospray. The ion source was equilibrated to ambient temperature. Mass spectra were collected in Sensitivity mode to maximize signal-to-noise. Argon gas was introduced into the Trap at a flow rate of 5 mL/min in all experiments. Trap/Transfer collision energy settings of 100/5 V, respectively, were used for all Nanodiscs. Nanodisc mass spectra were collected for 20 min and the continuously collected data were summed. All mass spectral data were processed without smoothing using MassLynx v. 4.1 (Waters Corp., Milford, MA, USA). The QTOF data shown in Supplementary Figure S3 were acquired using similar conditions described in detail in reference 1 of the main text.

Fourier Transform-Ion Cyclotron Resonance (FT-ICR) (UCLA, Los Angeles, CA, USA). All FT-ICR native-MS experiments were performed using SolariX 15 Tesla instrument (Bruker Daltonics, Billerica, MA, USA). The nESI capillary voltage was set to 0.6 to 0.8 kV in positive ionization mode. The temperature of drying gas was 100 °C and the flow rate was 2.5 L/min. The RF amplitude of the ion-funnels was 300 V peak-to-peak, and the applied voltages were 210 V and 6 V for funnels 1 and 2, respectively. The voltage of skimmer 1 was 50 and the skimmer 2 voltage was 20 V. The lowest values of RF frequencies were used in all ion-transmission

regions: multipole 1 (2 MHz), quadrupole (1.4 MHz), and transfer hexapole (1MHz). Ions were accumulated for 500 ms in the hexapole collision cell before being transmitted to the infinity ICR cell. A time-of-flight of 2.5 ms was used. Vacuum pressures for different regions were: source 2 mbar; quadrupole $2\times10^{-6}$ mbar; ultra-high vacuum chamber $2.6\times10^{-9}$ mbar. To assist in ion desolvation, mild collision-induced dissociation (CID) was performed in the hexapole collision cell by collision with argon at a voltage of 4 V. 1000 scans were averaged for each spectrum using 256,000 data points (transient length 0.085 s) per scan in magnitude mode. The MS Control software was Compass solariXcontrol, version 1.5.0, build 103, and the data were apodized using a full-sine-bell function. The mass spectrometer was externally calibrated with a 50 μg/mL solution cesium iodide in 1:1 (vol:vol) acetonitrile:water over the $m/z$ range 100 to 20,000.

**Results and Discussion**

Characterizing peak width and unresolved adductions in mass spectrum for non-Gaussian peak shapes. In the case that the mass spectral peak shape is unknown and not Gaussian, for example, when there is a long, asymmetric "tail" on each peak in the mass spectrum due to unresolved adductions of small ions or solvent molecules, the amplitude of the zero-frequency peak in the Fourier spectrum is not uniquely determine by the value of P($k$) at the harmonic peaks. This can result in gross errors in estimating mass spectral peak width when the zero-frequency amplitude for a particular charge state is not known. This scenario is demonstrated for a single charge state in Supplementary Figures S7C and S7D, where a sawtooth wave function is used as a model of a highly asymmetric peak shape. Because the zero-frequency component is in general needed to uniquely reconstruct asymmetric peaks, the Gaussian fit to P($k$) is

unsurprisingly poor. This example illustrates the potential danger of determining peak shape characteristics when the mass spectral peaks have highly asymmetric or unknown shapes.

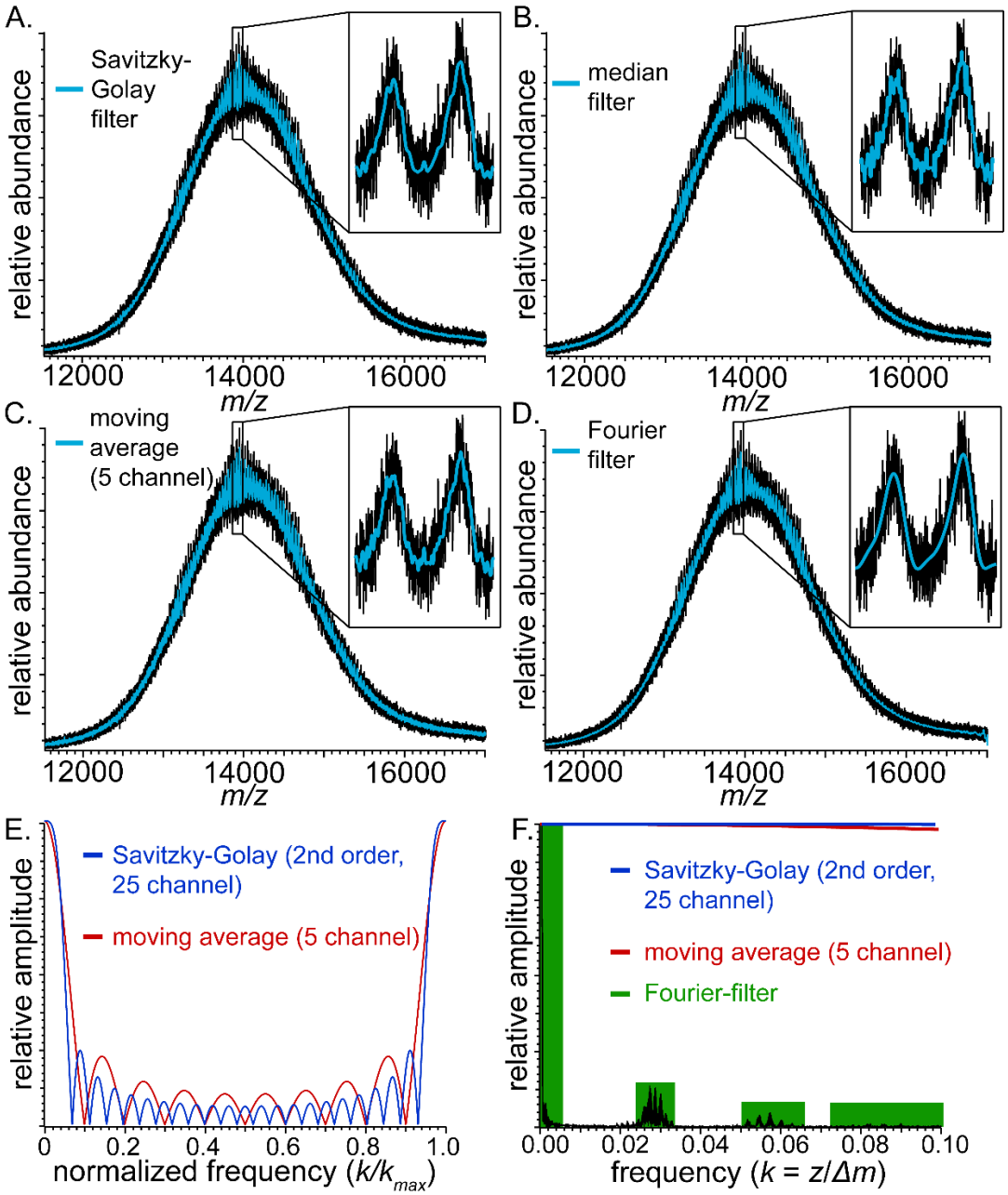


**Supplementary Figure S1**. Comparison of DMPC-MSP1D1 Nanodisc mass spectrum (black traces) acquired using QTOF mass spectrometer and processed (blue traces) using different types of filtering/smoothing algorithms (A-D). Panel E shows the FT representation of Savitzky-Golay and moving-average filter functions over the entire Fourier domain. Panel F shows the FT representation of Savitzky-Golay and moving-average filters (colored lines) and Fourier-filtered data (highlighted in green) for the Nanodisc mass spectrum. The Savitzky-Golay and moving-average filters have the effect of damping very high-frequency noise and slightly altering relative Fourier-domain peak amplitudes. By contrast, the Fourier filter removes all low-frequency noise between each set of harmonics and all high-frequency noise beyond the highest-harmonic data used without altering the relative amplitudes of the preserved data.

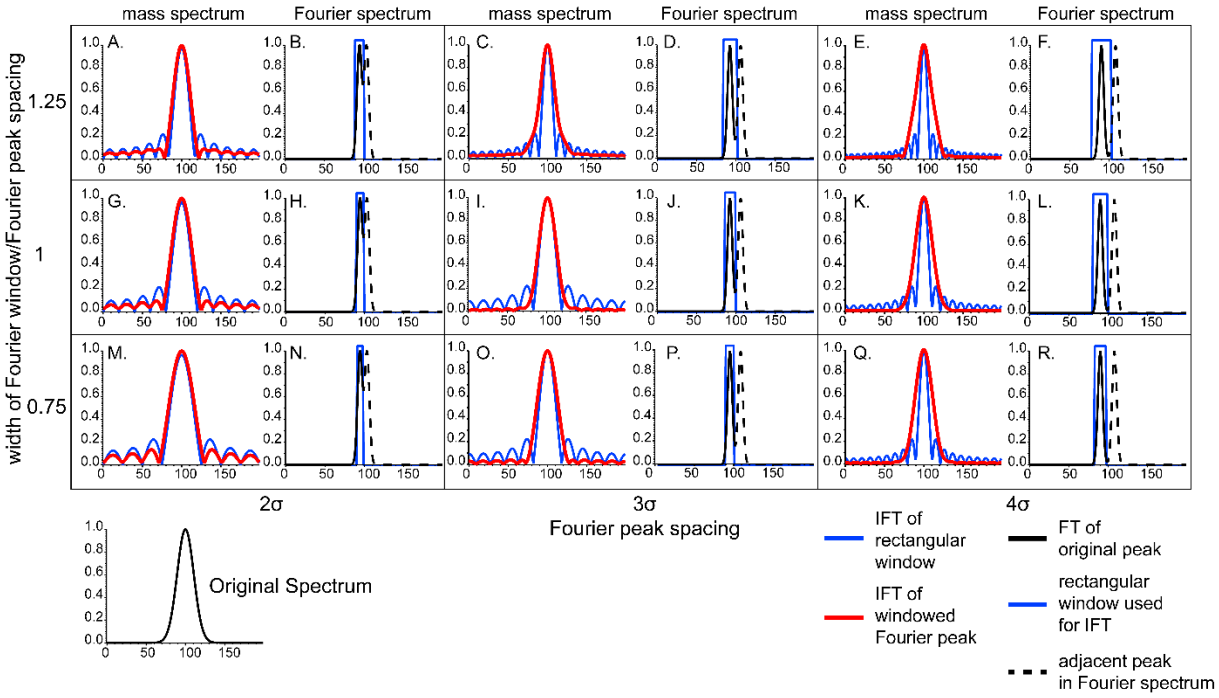


**Supplementary Figure S2.** Model mass spectral envelopes (A, C, E, G, I, K, M, O, Q; black traces) and corresponding Fourier spectra (B, D, F, H, J, L, N, P, R; left peak of each peak pair), illustrating effects of overlap of a Fourier-domain peak with an adjacent peak and choice of window width used in IFT. Peaks in Fourier domain have fixed standard deviation (σ), but spacing between Fourier-domain peaks varies from left to right as indicated. Width of Fourier-domain window (blue boxes) used for IFT to reconstruct mass spectral envelopes (red traces) varies as indicated along vertical axis, and blue trace in mass spectra indicate the IFT of the rectangular window function itself. Faithfulness of reconstructed mass spectral envelope generally increases from bottom left to top right, as the spacing between Fourier-domain peaks and the width of the window used for IFT increases. Windowing and overlap artifacts are less than 5% of the mass spectral peak abundance when the spacing between Fourier-domain peaks is at least 3 times their width (measured as standard deviation, σ).

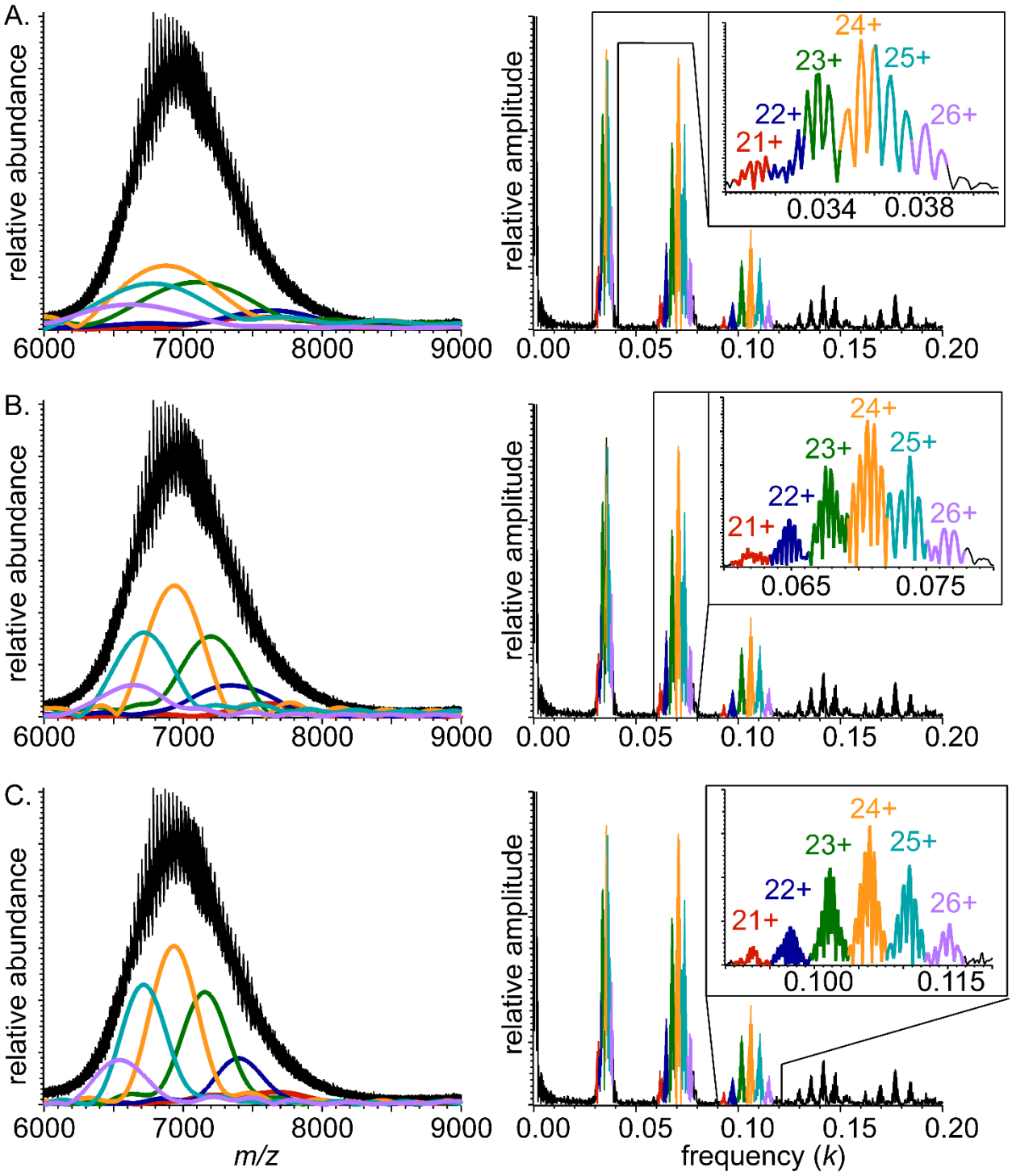


**Supplementary Figure S3.** Mass spectra (left) and corresponding Fourier spectra (right) for DMPC-MSP1D1 Nanodiscs acquired using QTOF mass spectrometer, showing reconstructed charge-state-specific mass spectral envelopes found using Fourier-domain (A) fundamentals, (B) second harmonics, and (C) third harmonics. Insets show detail for Fourier-domain peaks, with reconstructed mass spectral envelopes corresponding to charge states labeled with the same color

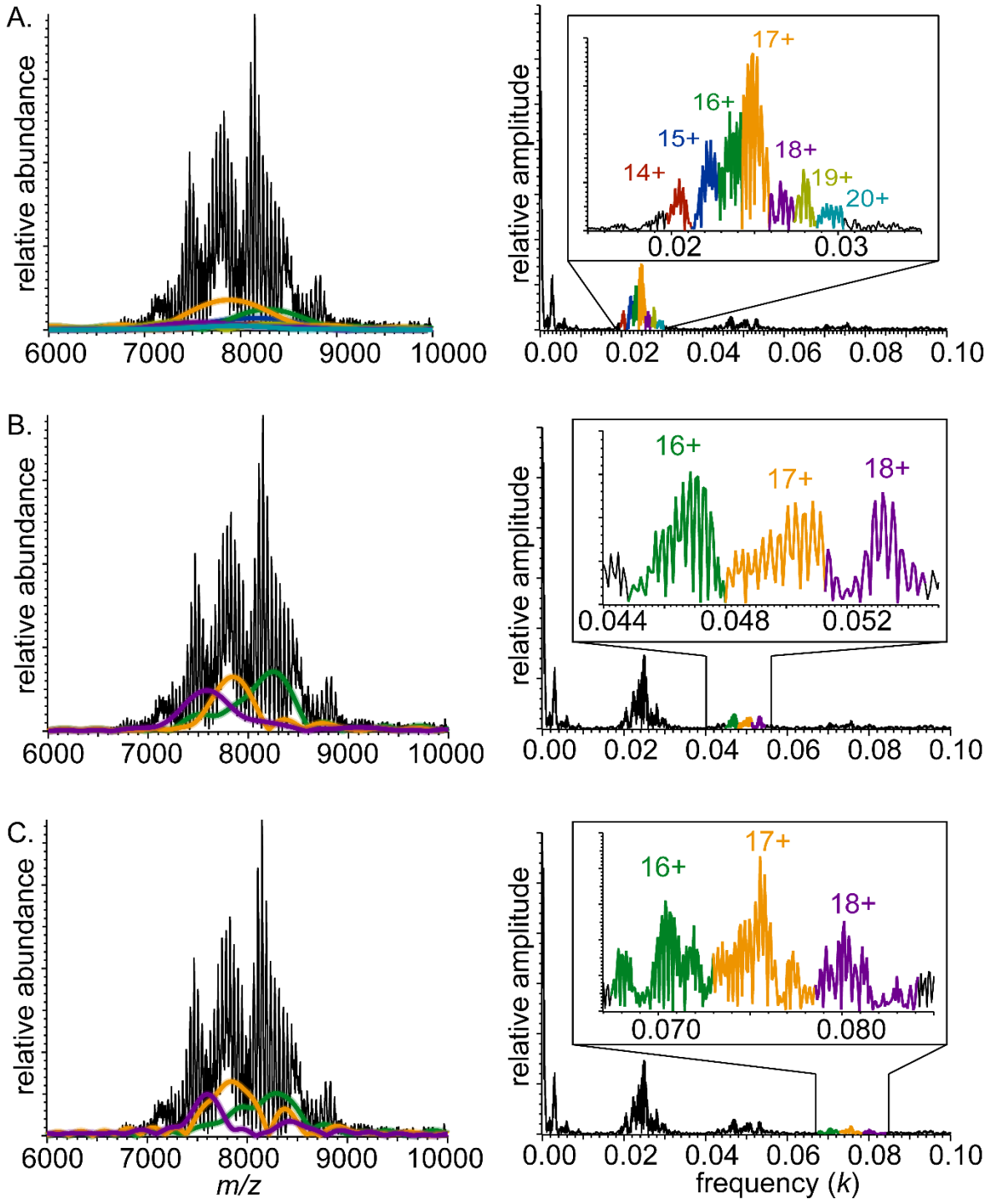


**Supplementary Figure S4.** Mass spectra (left) and corresponding Fourier spectra (right) for DMPC-MSP1D1 Nanodiscs acquired using FT-ICR mass spectrometer, showing reconstructed charge-state-specific mass spectral envelopes found using Fourier-domain (A) fundamentals, (B) second harmonics, and (C) third harmonics. Insets show detail for Fourier-domain peaks, with reconstructed mass spectral envelopes corresponding to charge states labeled with the same color

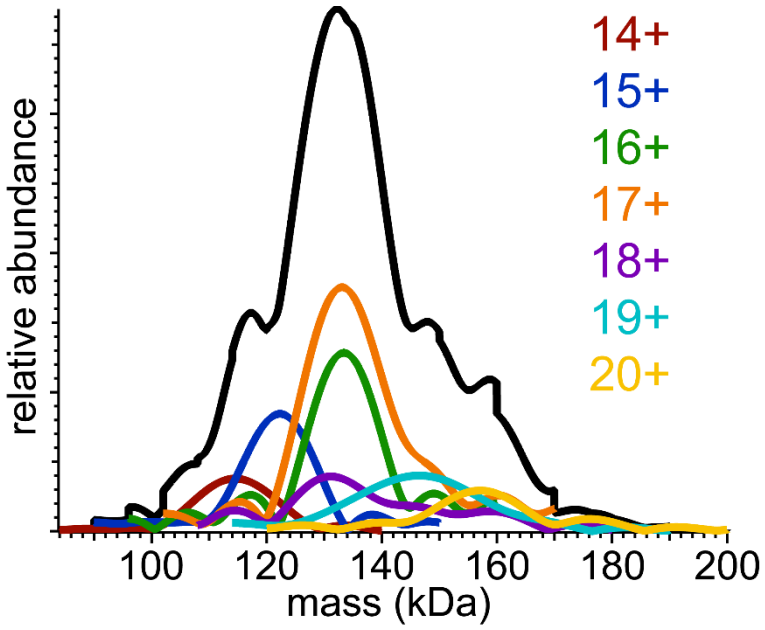


**Supplementary Figure S5.** Reconstructed zero-charge mass spectrum of DMPC-MSP1D1 Nanodiscs acquired on an FT-ICR mass spectrometer using data from Fourier-domain fundamental peaks for individual charge states (colored traces) and for entire ion population (black trace). Higher harmonics were not used for full ion population reconstruction because charge states other than 16-18+ had poor 2$^{nd}$ and 3$^{rd}$ harmonic signal-to-noise in the Fourier spectrum. Very broad mass distributions are attributed in part to artifacts from overlapped fundamental peaks (see Supplementary Figure S4; Supplementary Figure S10C and S10F contain a zero-charge mass spectrum reconstruction using the fundamentals, 2$^{nd}$, and 3$^{rd}$ harmonic peaks for the 16-18+ charge states)

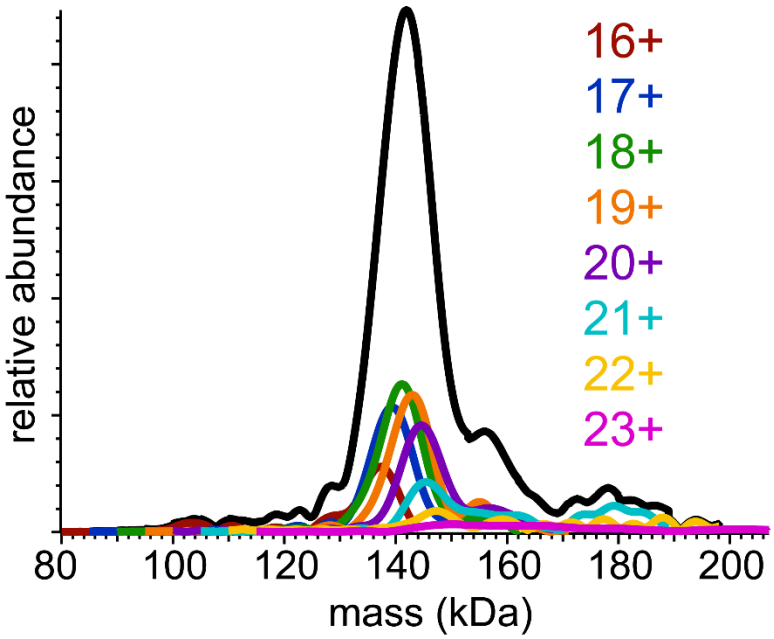


**Supplementary Figure S6.** Reconstructed zero-charge mass spectrum of DMPC-MSP1D1 Nanodiscs acquired on an Orbitrap mass spectrometer using data from Fourier-domain 2$^{nd}$ harmonic peaks for individual charge states (colored traces) and for entire ion population (black trace). Narrower mass distribution than that shown in Supplementary Fig. S5 is attributed to greater resolution of 2$^{nd}$ harmonic peaks for these data

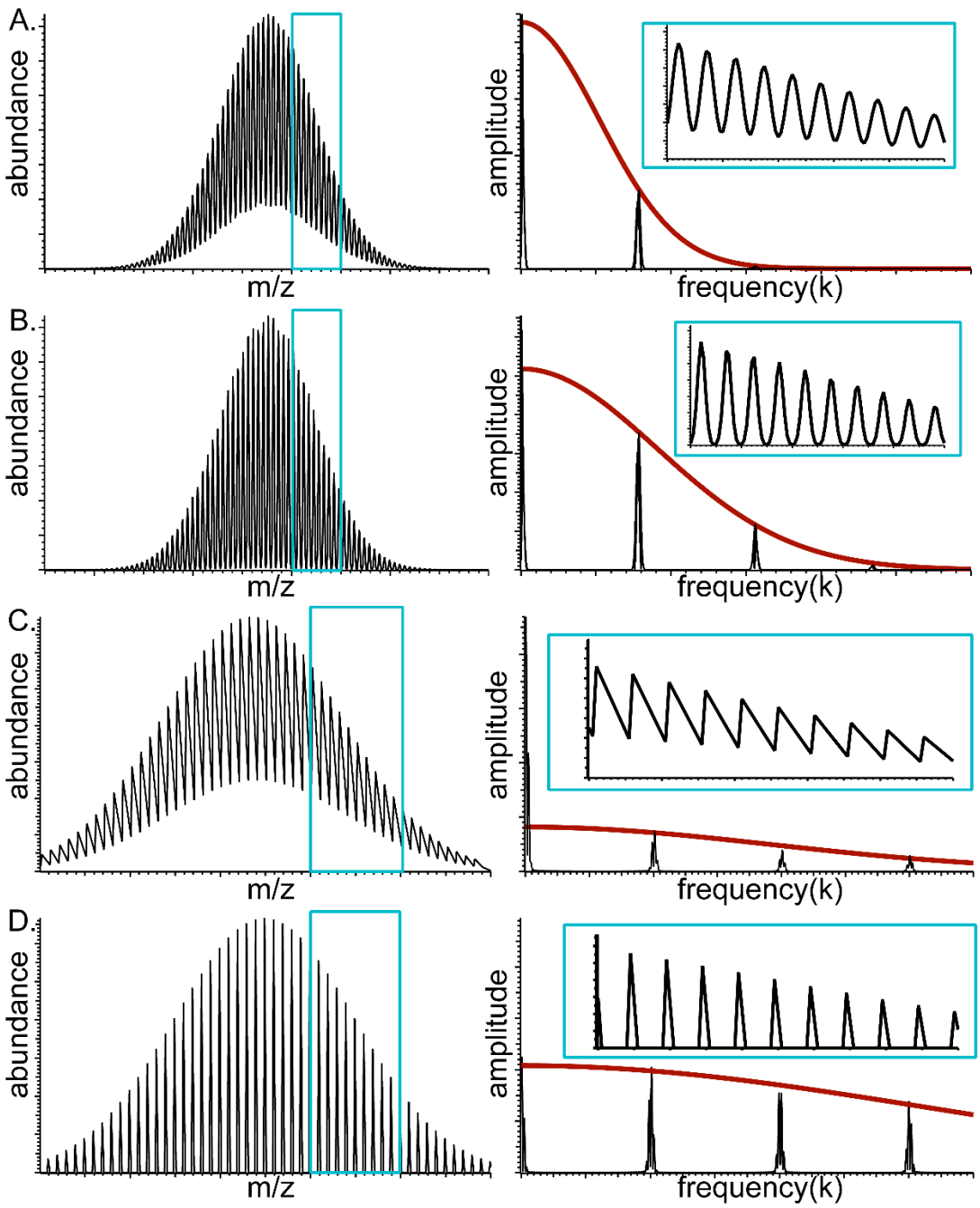


**Supplementary Figure S7.** Model mass spectrum (left) for a single charge state of a population of assembly ions that varies in the number of subunits, and the corresponding Fourier spectrum (right) for different peak shapes: (A) overlapping Gaussian peaks with a large curved baseline, (B) baseline-resolved Gaussian peaks, (C) overlapping sawtooth-shaped peaks with a large curved baseline, and (D) baseline-resolved sawtooth-shaped peaks. Insets shows close-up view of mass spectra. Gaussian fits to Fourier-domain decay functions, P(k), shown in red, are better for Gaussian-shaped mass spectral peaks than for poorly resolved sawtooth-shaped mass spectral peaks

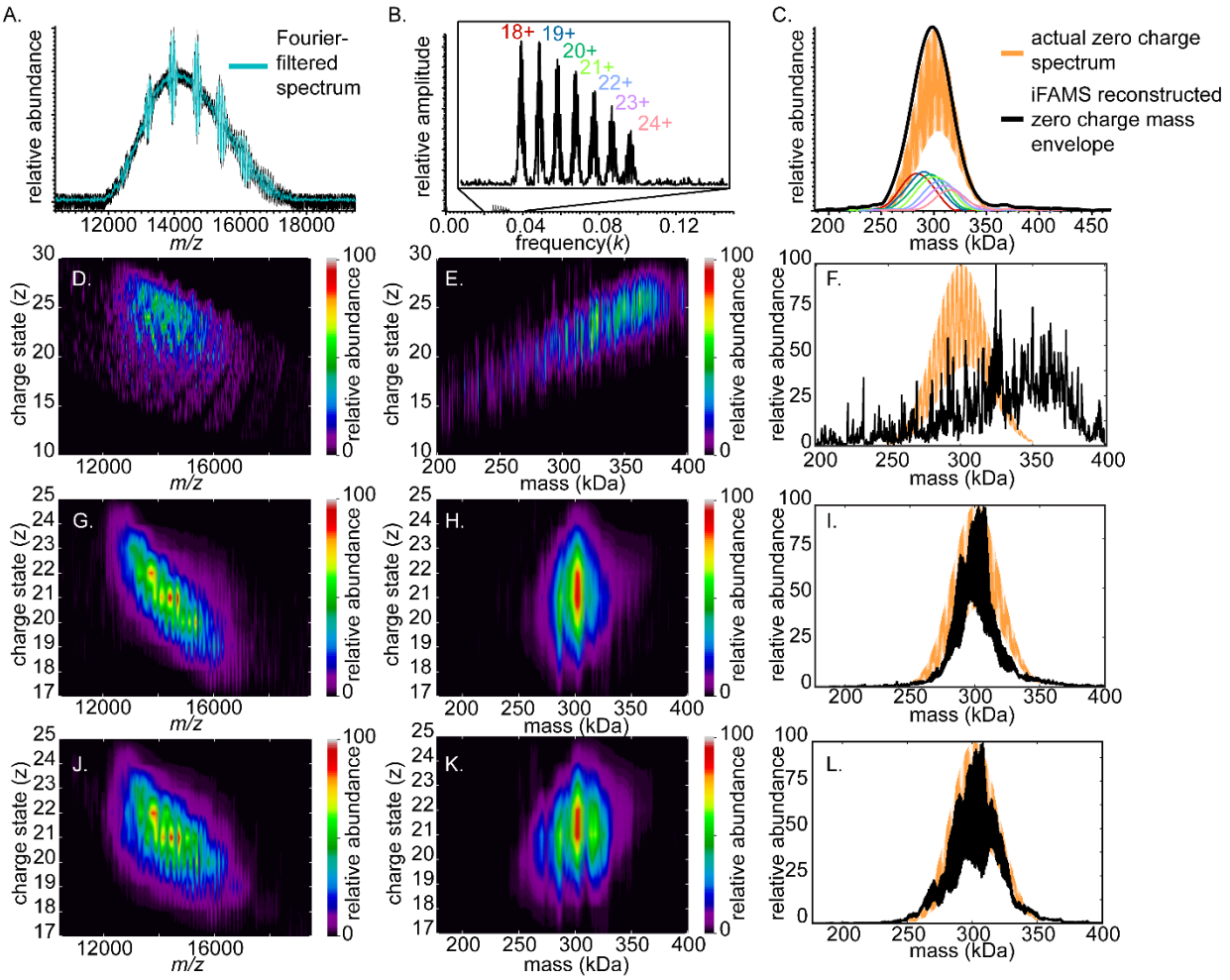


**Supplementary Figure S8.** Simulated mass spectrum with 20:1 signal-to-white-noise (A, black trace) for DPPC-MSP1E3D1 Nanodiscs with charge states 18-24+ and ~300-340 lipids, with the average number of lipids increasing by 10 with each increasing charge state, similar to experimental data. The blue trace in panel A shows the Fourier-filtered spectrum reconstructed using the Fourier-Transformed data from panel B (inset: fundamental peaks). Panel C shows the reconstructed zero-charge mass spectral envelopes for each charge state (colors of traces correspond to the charge states shown in panel B) the total zero-charge mass spectral envelope (black trace), and the exact zero-charge mass spectrum (orange trace). The reconstructions are remarkably accurate despite the low signal-to-noise of the input mass spectrum. Panels D, E, and F show deconvolution results from UniDec with a wide input charge state range (10-30+). Panels G, H, and I show deconvolution results from UniDec with a narrow input charge state range (17-25+) based on charge states identified using iFAMS. Panels J, K, and L show deconvolution results from UniDec using Fourier-filtered data from iFAMS and input charge state range 17-25+. Dramatic improvement of both the charge-state-specific and zero-charge mass spectra is observed when using output from iFAMS in UniDec.

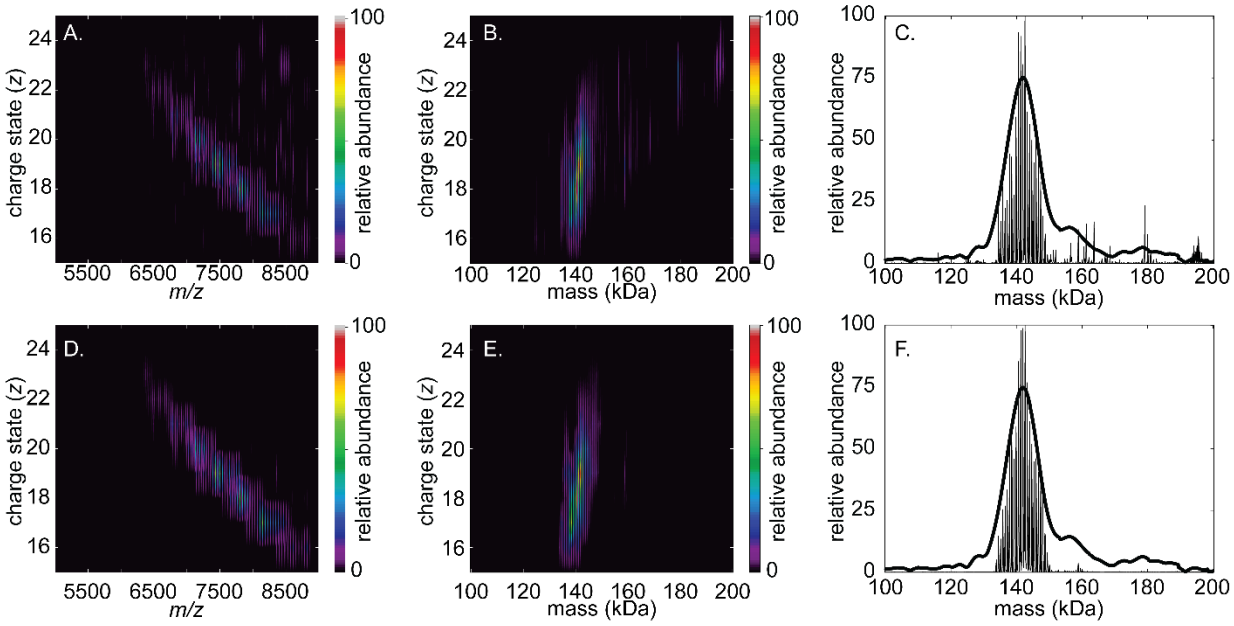


**Supplementary Figure S9.** Charge vs. *m/z* (left), charge vs. mass (middle) and total zero-charge mass spectrum (right) for mass spectrum of DMPC-MSP1D1 Nanodiscs acquired using Orbitrap mass spectrometer and deconvolved using UniDec. A, B, and C result from using "naive" input parameters for subunit mass, charge state range, peak width, and total mass, whereas D, E, and F result from using input parameter values obtained using the FT-based method described in the text. Smooth black trace in C and F represents zero-charge mass spectrum reconstructed from Fourier spectrum 2$^{nd}$ harmonics using iFAMS

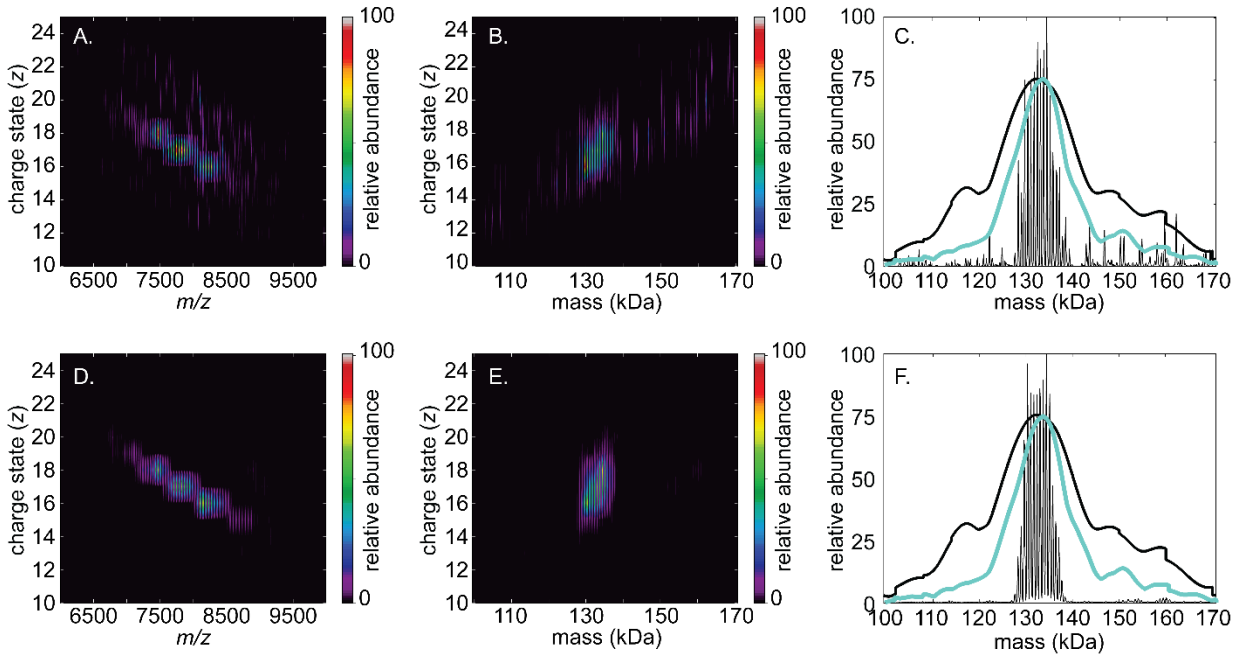


**Supplementary Figure S10.** Charge vs. *m/z* (left), charge vs. mass (middle) and total zero-charge mass spectrum (right) for mass spectrum of DMPC-MSP1D1 Nanodiscs acquired using FT-ICR mass spectrometer and deconvolved using UniDec. A, B, and C result from using "naive" input parameters for subunit mass, charge state range, peak width, and total mass, whereas D, E, and F result from using input parameter values obtained using the FT-based method described in the text. Smooth black (resp., blue) trace in C and F represents zero-charge mass spectrum reconstructed from Fourier spectrum fundamentals (resp., fundamentals, 2$^{nd}$, and 3$^{rd}$ harmonics for 16-18+ charge states) using iFAMS. (Charge states other than 16-18+ had poor 2$^{nd}$ and 3$^{rd}$ harmonic signal-to-noise in the Fourier spectrum.)

**Supplementary Table 1**. Lipid Mass, Charge States, and Lipid Stoichiometry Statistics Determined for Native-Like Nanodisc Ions Using FT-Based Approach.

| **Analyte (Instrument)** | **Harmonic** | **Measured Sub-unit Mass (Da)** | ***z*** | **Lipid Stoichiometry** |
|---|---|---|---|---|
| DPPC-MSP1E3D1 (QTOF) | Fundamental | 733. ± 2. | 18 | 273 ± 36† |
| | | | 19 | 290 ± 32† |
| | | | 20 | 304 ± 28† |
| | | | 21 | 316 ± 29† |
| | | | 22 | 325 ± 30† |
| | | | 23 | 340 ± 41† |
| | | | 24 | 353 ± 47 |
| | 2nd | 733.0 ± 0.8 | 18 | 275 ± 41* |
| | | | 19 | 294 ± 29 |
| | | | 20 | 305 ± 26 |
| | | | 21 | 315 ± 26 |
| | | | 22 | 327 ± 33 |
| | | | 23 | 352 ± 46* |
| | | | 24 | 383 ± 56* |
| | Average of fundamental and 2nd harmonic | N/A | 18 | 274 ± 39 |
| | | | 19 | 292 ± 31 |
| | | | 20 | 304 ± 27 |
| | | | 21 | 316 ± 28 |
| | | | 22 | 326 ± 32 |
| | | | 23 | 346 ± 45 |
| | | | 24 | 372 ± 55 |
| DMPC-MSP1D1 (QTOF) | Fundamental | 516.3 ± 15.5 (directly from Fourier spectrum) | 16 | 137 ± 18 |
| | | | 18 | 150 ± 22 |
| | Fundamental | 678 (input manually) | 21 | 169 ± 17† |
| | | | 22 | 180 ± 21† |
| | | | 23 | 179 ± 20† |
| | | | 24 | 185 ± 21† |
| | | | 25 | 196 ± 25† |
| | | | 26 | 197 ± 23† |

| | | | | |
|---|---|---|---|---|
| | 2nd | 679.2 ± 1.4 | 21 | 167 ± 14† |
| | | | 22 | 171 ± 15† |
| | | | 23 | 178 ± 16† |
| | | | 24 | 184 ± 17† |
| | | | 25 | 192 ± 22† |
| | | | 26 | 197 ± 22† |
| | 3rd | 678.3 ± 0.6 | 21 | 165 ± 17* |
| | | | 22 | 174 ± 13 |
| | | | 23 | 177 ± 12 |
| | | | 24 | 182 ± 13 |
| | | | 25 | 186 ± 16 |
| | | | 26 | 196 ± 23 |
| DMPC-MSP1D1 (FT-ICR) | Fundamental | 680.6 ± 4.7 | 14 | 101 ± 13†* |
| | | | 15 | 110 ± 15† |
| | | | 16 | 125 ± 19† |
| | | | 17 | 132 ± 17† |
| | | | 18 | 141 ± 24† |
| | | | 19 | 152 ± 19† |
| | | | 20 | 167 ± 22† |
| | 2nd | 637.8 ± 3.8 (directly from Fourier spectrum) | 15 | 121 ± 14 |
| | | | 16 | 129 ± 15 |
| | | | 17 | 136 ± 15 |
| | | 678 (input manually) | 16 | 125 ± 14 |
| | | | 17 | 133 ± 15 |
| | | | 18 | 139 ± 16 |
| | 3rd | 597.9 ± 2.4 (directly from Fourier spectrum) | 14 | 115 ± 15 |
| | | | 15 | 125 ± 15 |
| | | | 16 | 135 ± 18 |
| | | 678 (input manually) | 16 | 127 ± 15 |
| | | | 17 | 132 ± 16 |
| | | | 18 | 141 ± 19 |
| DMPC-MSP1D1 (Orbitrap) | Fundamental | 678.5 ± 3.6 | 16 | 125 ± 15† |
| | | | 17 | 129 ± 24† |
| | | | 18 | 137 ± 19† |

| | | | |
|---|---|---|---|
| | | 19 | 143 ± 22† |
| | | 20 | 149 ± 20† |
| | | 21 | 158 ± 22† |
| | | 22 | 166 ± 23 |
| | | 23 | 179 ± 23 |
| 2nd | 678.2 ± 1.0 | 16 | 128 ± 17 |
| | | 17 | 136 ± 14 |
| | | 18 | 143 ± 12 |
| | | 19 | 146 ± 14 |
| | | 20 | 150 ± 16 |
| | | 21 | 154 ± 20 |
| | | 22 | 162 ± 25 |
| | | 23 | 178 ± 28 |
| 3rd | 677.3 ± 1.2 | 16 | 127 ± 17 |
| | | 17 | 137 ± 12 |
| | | 18 | 141 ± 12 |
| | | 19 | 145 ± 12 |
| | | 20 | 150 ± 15 |
| | | 21 | 167 ± 24† |

* indicates harmonic peaks with signal-to-noise less than 10:1

† indicates harmonic peaks spaced by less than 1.5 times the sum of their apparent standard deviations